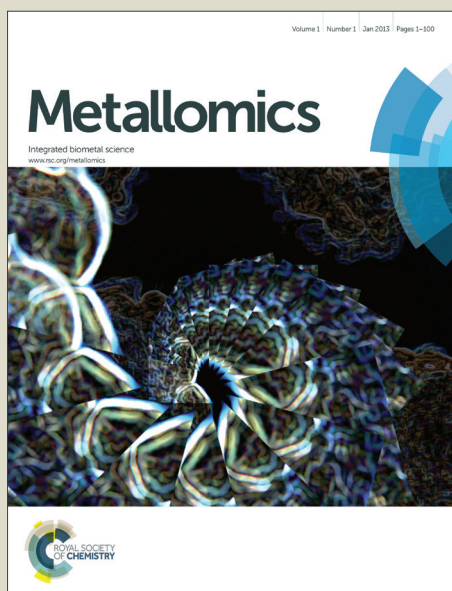


# Metallomics

Accepted Manuscript



This is an *Accepted Manuscript*, which has been through the Royal Society of Chemistry peer review process and has been accepted for publication.

*Accepted Manuscripts* are published online shortly after acceptance, before technical editing, formatting and proof reading. Using this free service, authors can make their results available to the community, in citable form, before we publish the edited article. We will replace this *Accepted Manuscript* with the edited and formatted *Advance Article* as soon as it is available.

You can find more information about *Accepted Manuscripts* in the [Information for Authors](#).

Please note that technical editing may introduce minor changes to the text and/or graphics, which may alter content. The journal's standard [Terms & Conditions](#) and the [Ethical guidelines](#) still apply. In no event shall the Royal Society of Chemistry be held responsible for any errors or omissions in this *Accepted Manuscript* or any consequences arising from the use of any information it contains.

[MT-ART-07-2014-000175](#)

**Experimental and density functional theory (DFT) methods studies on the interactions of Ru(II) polypyridyl complexes with the RAN triplex poly(U)•poly(A)\*poly(U)**

Hong Zhang,<sup>a</sup> Xuewen Liu,<sup>b</sup> Xiaojun He,<sup>a</sup> Ying liu,<sup>a</sup> and Lifeng Tan<sup>\*c</sup>

<sup>a</sup> College of Chemistry, Xiangtan University, Xiangtan 411105, China

<sup>b</sup> Department of Chemistry and Chemical Engineering, Hunan University of Arts and Science, Changde 415000, PR China

<sup>c</sup> Key Lab of Environment-friendly Chemistry and Application in Ministry of Education, Xiangtan University, Xiangtan 411105, China

E-mail: lfwyxh@yeah.net; Fax: +86-731-5829-2251; Tel: +86-731-5829-3997

There is renewed interest in investigating triple helices because these novel structures have been implicated as a possible means of controlling cellular processes by endogenous or exogenous mechanisms. Due to the Hoogsteen base pairing, triple helices are, however, thermodynamically less stable than the corresponding duplexes. The poor stability of triple helices limits their practical applications under physiological conditions. In contrast to DNA triple helices, small molecules stabilizing RNA triple helices at present are less well established. Furthermore, most of these studies are limited to organic compounds and, to a far lesser extent, on metal complexes. In this work, two Ru(II) complexes,  $[\text{Ru}(\text{bpy})_2(\text{btip})]^{2+}$  (Ru1) and  $[\text{Ru}(\text{phen})_2(\text{btip})]^{2+}$  (Ru2), have been synthesized and characterized. The binding properties of the two metal complexes with the triple RNA poly(U)•poly(A)\*poly(U) were studied by various biophysical and density functional theory methods. The main results obtained here suggest that the slight binding difference in Ru1 and Ru2 may be attributed to

1  
2 the planarity of the intercalative ligand and the LUMO level of Ru(II) complexes. This study  
3  
4 further advances our knowledge on the triplex RNA-binding by metal complexes, particularly  
5  
6  
7 Ru(II) complexes.  
8  
9

## 10 11 **1. Introduction**

12  
13 Nucleic acid triple helices (also called triplexes), containing triple-strand DNA-type and  
14  
15 RNA-type structures, have attracted considerable attention in recent years.<sup>1-5</sup> The reason for  
16  
17 this is that these novel structures have been implicated as a possible means of controlling  
18  
19 cellular processes by endogenous or exogenous mechanisms. Stabilization of triplexes is  
20  
21 extremely important for carrying out their biological functions,<sup>6</sup> such as antigene therapy and  
22  
23 gene regulation. Due to the Hoogsteen base pairing, triplexes are, however,  
24  
25 thermodynamically less stable than the corresponding duplexes. The poor stability of these  
26  
27 structures limits their use under physiological conditions.<sup>6,7</sup> In this regard, small molecules  
28  
29 able to stabilize the specific sequences of triplexes are of very importance.<sup>8</sup>  
30  
31  
32  
33  
34  
35

36  
37 In recent years, many efforts are under way to use natural and synthetic small molecules to  
38  
39 modulate the properties of triplex structures under physiological conditions.<sup>9-11</sup> In contrast to  
40  
41 DNA triple helices, however, investigations of small molecules stabilizing RNA triple helices  
42  
43 at present are less well established. Furthermore, most of these studies are limited to organic  
44  
45 compounds<sup>12-14</sup> and, to a far lesser extent, on metal complexes.<sup>15-17</sup> In general, the  
46  
47 stabilization of RNA triple helices can be achieved by the action of intercalators,<sup>18,19</sup> in  
48  
49 particular when covalently linked to the third strand.<sup>20</sup> However, intercalators not covalently  
50  
51 linked can either stabilize or destabilize RNA triplexes.<sup>21,22</sup> For example, the melting  
52  
53 experiments reveal that proflavine (PR) and its platinum(II)-proflavine complex (PtPR)<sup>15</sup> and  
54  
55  
56  
57  
58  
59  
60

1  
2 ethidium<sup>23</sup> tend to destabilize the triplex, whereas berberine analogs<sup>13</sup> are able to strongly  
3  
4 stabilize the Hoogsteen base paired third strand of RNA triplexes by intercalation. In addition,  
5  
6 some alkaloids stabilize the Hoogsteen base-paired third strand of RNA triplexes almost  
7  
8 without affecting the stability of the duplex, such as berberine, palmatine and coralyne.<sup>18</sup>  
9  
10 Interestingly, studies of the interaction mechanisms of coralyne with  
11  
12 poly(U)•poly(A)\*poly(U) (Fig. 1, where •denotes the Watson-Crick base pairing and \*  
13  
14 denotes the Hoogsteen base pairing) reflect that coralyne tends to stabilize the triplex structure  
15  
16 because of this small molecule being able to induce the triplex-to-duplex conversion and also  
17  
18 the duplex-to-triplex conversion. These researches reveal that the intercalative process and  
19  
20 modes effect on the stability of RNA triple helices are more complicated than previously  
21  
22 thought and very sensitive to the structure of the bound compound.<sup>14b</sup> In our quest for small  
23  
24 molecules to improve the stabilization of RNA triplexes, we recently reported a Ru(II)  
25  
26 polypyridyl complex, [Ru(phen)<sub>2</sub>(mdpz)]<sup>2+</sup> {phen = 1,10-phenanthroline, mdpz  
27  
28 =7,7'-methylenedioxyphenyl-dipyrido-[3,2-*a*:2',3'-*c*]-phenazine}, could serve as a prominent  
29  
30 molecular “light switch” for poly(U)•poly(A)\*poly(U) under physiological conditions and  
31  
32 enhance the triplex stabilization through intercalation.<sup>16</sup> This complex is also a first emission  
33  
34 ‘light switch’ for RNA triplexes.  
35  
36  
37  
38  
39  
40  
41  
42  
43  
44

45 To further evaluate and understand the factors effect on the stability of RNA triplexes, it is  
46  
47 quite necessary and really significant to study the interactions between RNA triplexes and  
48  
49 small molecules with different shapes and electronic properties. It’s well established that Ru(II)  
50  
51 polypyridyl complexes, due to a combination of easily constructed rigid chiral structures  
52  
53 spanning all three spatial dimensions and a rich photophysical repertoire, prominent DNA  
54  
55 binding properties and promising biological activity, have attracted considerable attentions in  
56  
57  
58  
59  
60

1  
2 recent years.<sup>24–26</sup> Unfortunately, the study of Ru(II) polypyridyl complex–RNA triplex  
3  
4 interactions is very scarce at present.<sup>15,16</sup>  
5  
6

7  
8 To explore the factors effect on the stabilization of RNA triplexes by octahedral Ru(II)  
9  
10 complexes,  $[\text{Ru}(\text{bpy})_2(\text{btip})]^{2+}$  {Ru1; btip = 2-benzo[*b*]thien-2-yl-1*H*-imidazo[4,5-*f*]-  
11  
12 [1,10]phenanthroline} and  $[\text{Ru}(\text{phen})_2(\text{btip})]^{2+}$  (Ru2; phen = 1,10-phenanthroline) (Fig. 1)  
13  
14 have been synthesized and characterized In this study. The binding properties of Ru1 and Ru2  
15  
16 with the triplex RNA poly(U)•poly(A)\*poly(U) have been explored by using biophysical  
17  
18 techniques and density functional theory (DFT) methods. The main results obtained here  
19  
20 further advance our knowledge on the binding of RNA triplexes with metal complexes,  
21  
22 particularly Ru(II) complexes.  
23  
24  
25  
26  
27

## 28 29 **2. Experimental Sections**

### 30 31 **2.1. Materials**

32  
33 1,10-phenanthroline-5,6-dione,<sup>27</sup> *cis*- $[\text{Ru}(\text{phen})_2\text{Cl}_2]\cdot 2\text{H}_2\text{O}$  and *cis*- $[\text{Ru}(\text{bpy})_2\text{Cl}_2]\cdot 2\text{H}_2\text{O}$ <sup>28</sup> were  
34  
35 prepared according to literature procedures. Polynucleotide samples of double stranded  
36  
37 poly(A)•poly(U) and single stranded poly(U) were obtained from Sigma-Aldrich Corporation  
38  
39 (St. Louis, MO, USA) and were used as received. The RNA triplex poly(U)•poly(A)\*poly(U)  
40  
41 was prepared as reported earlier.<sup>16</sup> The concentration of poly(U)•poly(A)\*poly(U) was  
42  
43 determined optically using molar extinction coefficients,  $\epsilon$  ( $\text{M}^{-1} \text{cm}^{-1}$ ) reported in the  
44  
45 literature.<sup>29–31</sup> All titration experiments were conducted at 20 °C in pH 7.0 phosphate buffer (6  
46  
47 mmol/L  $\text{Na}_2\text{HPO}_4$ , 2 mmol/L  $\text{NaH}_2\text{PO}_4$ , 1 mmol/L  $\text{Na}_2\text{EDTA}$ , 19 mmol/L  $\text{NaCl}$ ).  
48  
49  
50  
51  
52  
53

### 54 55 **2.2. Physical measurement**

56  
57 Microanalyses (C, H and N) were carried out on a Perkin–Elmer 240Q elemental analyzer. <sup>1</sup>H  
58  
59  
60

1  
2 NMR spectra were recorded on an Avance-400 spectrometer with  $d_6$ -DMSO as solvent at  
3  
4 room temperature and TMS (tetramethylsilane) as the internal standard. Mass Spectrometer  
5  
6 was performed on an Autoflex III™ Maldi-Tof mass spectrometer (Bruker) using DMSO as  
7  
8 the mobile phase. UV-visible spectra were recorded on a Perkin-Elmer Lambda-25  
9  
10 spectrophotometer, and emission spectra were recorded on a Perkin-Elmer LS-55  
11  
12 luminescence spectrometer at room temperature. Circular dichroism (CD) spectra were  
13  
14 measured on a JASCO-810 spectropolarimeter.  
15  
16  
17  
18  
19

### 20 21 **2.3. Synthesis of 2-benzo[*b*]thien-2-yl-1*H*-imidazo[4,5-*f*][1,10]phenanthroline (btip)**<sup>32</sup>

22  
23 A mixture of 1,10-phenanthroline-5,6-dione (0.16 g, 0.5 mM), benzo[*b*]thiophene-2-  
24  
25 carbaldehyde (0.07 g, 1.0 mM), ammonium acetate (1.54 g, 20 mM), and glacial AcOH (10 ml)  
26  
27 was heated at reflux with stirring for 1.5 h. The cooled solution was filtered and diluted with  
28  
29 water, then neutralized with concentrated aqueous ammonia. The yellow precipitate was  
30  
31 collected and purified by column chromatography (Alox; EtOH/toluene 5:1) to afford btip  
32  
33 (0.17 g, 96%). Maldi-Tof-MS (*m/z*): 492.2 [M+1]. Anal. calc. for C<sub>21</sub>H<sub>12</sub>N<sub>4</sub>S: C 71.57, H 3.43,  
34  
35 N 15.90; found: C 71.35, H 3.57, N 15.74.  
36  
37  
38  
39  
40

### 41 **2.4. Synthesis of [Ru(bpy)<sub>2</sub>(btip)](ClO<sub>4</sub>)<sub>2</sub>·H<sub>2</sub>O (Ru1)**<sup>32</sup>

42  
43 A mixture of *cis*-[Ru(bpy)<sub>2</sub>Cl<sub>2</sub>]·2H<sub>2</sub>O (104 mg, 0.20 mM), btip (71 mg, 0.20 mM), and  
44  
45 ethylene glycol (20 ml) was thoroughly deoxygenated. The purple mixture was heated for 8 h  
46  
47 at 150 °C under argon atmosphere. When the solution finally turned red, it was cooled to room  
48  
49 temperature and equal volume of saturated aqueous sodium perchlorate solution was added  
50  
51 under vigorous stirring. The red solid was collected and washed with small amounts of H<sub>2</sub>O,  
52  
53 EtOH, and Et<sub>2</sub>O, respectively. After that, the red solid was dried under vacuum and purified on  
54  
55  
56  
57  
58  
59  
60

a neutral alumina column with MeCN/toluene (2:1, v/v) to afford the title complex (143 mg, 73%). Maldi-Tof-MS (m/z): 765.1 ([M-2ClO<sub>4</sub>-H]<sup>+</sup>). Anal. calc. for C<sub>41</sub>H<sub>30</sub>Cl<sub>2</sub>N<sub>8</sub>O<sub>9</sub>RuS: C 50.11, H 3.08, N 11.40; found: C 50.02, H 3.10, N 11.39. <sup>1</sup>H NMR (400 MHz, ppm, D<sub>6</sub>-DMSO; d, doublet; s, singlet; t, triplet; m, multiplet): 8.95 (d, J = 7.6, 2H), 8.85 (dd, J<sub>1</sub> = 8.8, J<sub>2</sub> = 8.8, 4H), 8.20 (t, 2H), 8.09 (t, 2H), 7.96 (d, J = 8.0, 1H), 7.91 (d, J = 6.4, 1H), 7.86 (d, J = 4.8, 2H), 7.78 (d, J = 7.2, 2H), 7.57 (t, 6H), 7.34–7.40 (m, 5H).

## 2.5. Synthesis of [Ru(bpy)<sub>2</sub>(pnip)](ClO<sub>4</sub>)<sub>2</sub>·H<sub>2</sub>O (Ru2)

The dark red complex [Ru(phen)<sub>2</sub>(btip)](ClO<sub>4</sub>)<sub>2</sub> was obtained by a similar procedure to that described above. Yield: 132 mg, 64%. Anal. Calcd for C<sub>45</sub>H<sub>30</sub>Cl<sub>2</sub>N<sub>8</sub>O<sub>9</sub>RuS: C, 52.43; H, 2.93; N, 10.87. Found: C, 52.35; H, 2.98; N, 10.82. Maldi-Tof-MS (m/z): 813.0 ([M-2ClO<sub>4</sub>-H]<sup>+</sup>). <sup>1</sup>H NMR (ppm, DMSO-d<sub>6</sub>, 400 MHz): 8.90 (d, J = 8.4, 2H); 8.75 (d, J = 8.0, 4H); 8.39 (d, J = 14.4, 4H); 8.09 (d, J = 4.8, 4H); 8.02 (s, 1H); 7.93 (d, J = 7.2, 2H); 7.88 (d, J = 8.0, 1H); 7.74–7.81 (m, 6H), 7.62 (t, 1H), 7.35 (dd, J<sub>1</sub> = 7.6, J<sub>2</sub> = 8.4, 2H).

## 2.6. RNA-binding experiments

The methods for spectroscopic titrations and viscosity measurements of the two Ru(II) complexes binding with poly(U).poly(A)\*poly(U) are the same as before.<sup>16</sup> The intrinsic binding constants (*K<sub>b</sub>*) and the binding site size (*s*) are determined the changes of absorbance at 463 nm for Ru1 and 464 nm for Ru2 by using the following equation.<sup>33</sup>

$$\frac{\mathcal{E}_a - \mathcal{E}_f}{\mathcal{E}_b - \mathcal{E}_f} = \frac{\sqrt{b - (b^2 - 2K_b^2 C_t [RNA] / s)}}{2K_b C_t} \quad (1a)$$

$$b = \frac{1 + K_b C_t + K_b [RNA]}{2s} \quad (1b)$$

where [RNA] is the concentration of poly(U).poly(A)\*poly(U) in the nucleotide phosphate and  $\mathcal{E}_a$ ,  $\mathcal{E}_f$  and  $\mathcal{E}_b$  are the apparent, free and bound metal complex extinction coefficients,

1  
2 respectively.  $K_b$  is the equilibrium binding constant in  $M^{-1}$ ,  $C_t$  is the total metal complex  
3  
4 concentration and  $s$  is the binding site size.  
5  
6

## 7 8 **2.7. Thermal denaturation studies**

9  
10 Thermal RNA denaturation experiments were carried out with a Perkin-Elmer Lambda-25  
11  
12 spectrophotometer equipped with a Peltier temperature-control programmer ( $\pm 0.1$  °C). The  
13  
14 temperature of the solution was increased from 20 to 60 °C at a rate of 1 °C  $min^{-1}$ , and the  
15  
16 absorbance at 260 nm was continuously monitored for solutions of the RNA Triplex (32.1  $\mu M$ )  
17  
18 in the absence and presence of different concentrations of either Ru1 or Ru2 in phosphate  
19  
20 buffer. The thermal melting temperature ( $T_m$ ) was taken as the midpoint of the melting  
21  
22 transition as determined by the maximal of the first derivative plot.<sup>15</sup>  
23  
24  
25  
26  
27

## 28 29 **3. Theoretical calculations**

30  
31 The structural schematic diagrams of Ru1 and Ru2 are shown in Fig. 1. The general structure  
32  
33 of each metal complex contains a Ru(II) ion, two ancillary ligands (bpy or phen) and a  
34  
35 intercalative ligand btip. There is not any symmetry in these complexes. All calculations have  
36  
37 been performed with the G98 quantum chemistry program-package,<sup>34,35</sup> at the DFT/B3LYP  
38  
39 level using 6-31G\* basis set on the carbon, nitrogen, sulfur and hydrogen atoms and a  
40  
41 LanL2DZ basis set<sup>36,37</sup> with effective core potential on the ruthenium atom. The full geometry  
42  
43 optimization computations for the ground states of these complexes with singlet state<sup>38</sup> were  
44  
45 carried out. In order to vividly depict the detail of the frontier molecular orbital interactions,  
46  
47 the stereographs of some related frontier molecular orbitals of the complexes were drawn with  
48  
49 the Molden v3.7 program<sup>39</sup> based on the computational results.  
50  
51  
52  
53  
54  
55  
56  
57  
58  
59  
60

### 3. Results and discussion

#### 3.1. Electronic absorption spectral studies of the binding

The application of electronic absorption spectroscopy in triplexes-binding studies is one of the most useful techniques.<sup>13-15</sup> Aromatic small molecules binding with triplexes through intercalation usually result in obvious hypochromism and bathochromism, which is attributed to  $\pi$ - $\pi$  stacking interactions between an aromatic chromophore of aromatic small molecules and the base pairs of triplexes.<sup>40</sup> The extent of the hypochromism commonly parallels the intercalative binding strength. Thus, the binding of Ru1 and Ru2 with poly(U)•poly(A)\*poly(U) was first performed by absorption spectral measurements.

The absorption spectra of Ru1 and Ru2 in the absence and presence of the RNA triplex are given in Fig. 2. Fig. 2 indicates that obvious hypochromisms and red shifts in the MLCT bands (MLCT = metal-to-ligand charge-transfer) of the two complexes are observed upon progressively increasing the concentration of the RNA triplex. In the case of Ru1, the hypochromism at 463 nm reached about 16.7% with a red shift of 6 nm at a [UAU]/[Ru] ratio of 6.28 {UAU stands for poly(U)•poly(A)\*poly(U), Ru stands for Ru1 and Ru2, respectively.}. For Ru2, the hypochromism at 464 nm was around 15.6%, with a red shift of 3 nm at a [UAU]/[Ru] ratio of 4.15. These spectral characteristics suggest that both complexes interact with the RNA triplex most likely through an intercalative mode, which involves a stacking interaction between the aromatic chromophore and the base pairs of the RNA triplex.

From the decay of the absorbance of the two complexes monitored at the MLCT bands, the intrinsic binding constants  $K_b$  of Ru1 and Ru2 were determined to be  $(2.23 \pm 0.41) \times 10^6$   $M^{-1}$  ( $s = 1.31 \pm 0.03$ ) and  $(1.59 \pm 0.46) \times 10^6$   $M^{-1}$  ( $s = 0.85 \pm 0.04$ ), respectively. The binding constants  $K_b$  and the binding site size  $s$  of Ru1 are slightly higher than those of Ru2, which

1  
2 suggests that Ru1 binding to the triplex RNA is stronger than Ru2. In addition, the  $K_b$  values  
3  
4 of the two complexes are much higher than those of the compounds binding with the triplex  
5  
6 RNA through a partial intercalation, such as the metal complex PtPR ( $1.3 \times 10^4 \text{ M}^{-1}$ ),<sup>15</sup>  
7  
8 alkaloid berberine [ $1.6 \pm 0.40) \times 10^5 \text{ M}^{-1}$ ]<sup>18</sup> and palmatine [ $(1.6 \pm 0.40) \times 10^5 \text{ M}^{-1}$ ].<sup>41</sup> These  
9  
10 indicate that the sizes and shapes of small molecules have significant effects on the binding  
11  
12 affinities  
13  
14  
15

### 16 17 18 **3.2. Spectrofluorimetric and studies**

19  
20 Information regarding the binding affinity of the two complexes toward the triplex can also be  
21  
22 obtained from emission spectroscopy. Fig. 3 shows the emission spectra of Ru1 and Ru2 in the  
23  
24 absence and presence of the RNA triplex poly(U)•poly(A)\*poly(U). The emission intensity of  
25  
26 either Ru1 or Ru2 increases steadily upon progressive addition the triplex RNA and eventually  
27  
28 reaches about 17 and 14 times in comparison with the triplex-free Ru1 and Ru2, respectively.  
29  
30 In each case, a large emission change is indicative of a strong association of the complex with  
31  
32 the triplex, resulting presumably from an effective overlap of the bound complex with the base  
33  
34 triplets.<sup>18</sup> The result further indicates that the location of the bound Ru1 and Ru2 in a  
35  
36 hydrophobic environment similar to an intercalated state and Ru1 protected by the triplex  
37  
38 RNA is more efficient compared with Ru2. Therefore, the accessibility of water molecules to  
39  
40 Ru1 in the presence of the triplex is more difficult in comparison with Ru1, resulting in Ru1  
41  
42 displaying a greater emission increase than Ru2 upon binding to the triplex in saturation state.  
43  
44  
45  
46  
47  
48  
49  
50

### 51 **3.3. Determination of the binding mode by viscosity studies**

52  
53  
54  
55  
56  
57  
58  
59  
60  
Viscometric technique is a reliable hydrodynamic method to clarify the binding modes of  
small molecules toward DNA/RNA.<sup>42</sup> The effects of Ru1 and Ru2 on the relative viscosity of

1  
2  
3 the RNA triplex poly(U)•poly(A)\*poly(U) are presented in Fig. 4. Upon addition of either Ru1  
4  
5 or Ru2 to the triplex, an initial decrease in the relative viscosity of the triplex solution was  
6  
7 observed and subsequent increases in the apparent molecular length of the triplex occurred.  
8  
9 The initial decrease in the apparent molecular length of the triplex may be indicative of a  
10  
11 conformational change in the triplex induced by either Ru1 or Ru2. Such a conformational  
12  
13 change may be attributed to a kink or bend of the helix induced by the complex, which thereby  
14  
15 reduces the effective molecular length of the triplex.<sup>43</sup> Upon the ratios of [Ru]/[UAU] further  
16  
17 increasing, the subsequent extensions of the length of the triplex may arise from the  
18  
19 intercalation effect. In addition, the increase in solution viscosity observed in the contour  
20  
21 length profile of the triplex may simply reflect a binding-induced increase in the stiffness of  
22  
23 the triplex by Ru1 and Ru2.  
24  
25  
26  
27  
28  
29

30 The above viscosity studies further confirm that Ru1 and Ru2 bind to the RNA triplex via  
31  
32 an intercalative mode. Notably, the effects of the two complexes on the viscosity of the RNA  
33  
34 triplex are obviously different from the metal complex PRPt.<sup>15</sup> Concerning PtPR, it binds the  
35  
36 triplex RNA poly(U)•poly(A)\*poly(U) through a partial intercalative mode, due to the  
37  
38 platinum-containing residues prevent full penetration of the PR residue between base planes,  
39  
40 which results in no obvious changes of the viscosity of poly(U)•poly(A)\*poly(U) upon  
41  
42 addition of PtPR. These data also indicates that the size and shape of metal complexes has a  
43  
44 significant effect on the binding modes.  
45  
46  
47  
48  
49

### 50 51 **3.4. Conformational change studies**

52  
53 To investigate the effect of Ru1 and Ru2 on the conformation of the RNA triplex, we also  
54  
55 recorded CD spectra of the triplex poly(U)•poly(A)\*poly(U) modified by Ru1 or Ru2 (Fig.  
56  
57  
58  
59  
60

1  
2  
3 5). Due to the stacking interactions between the base triplets and the helical structure of  
4  
5 the triplex strands, the intrinsic CD spectra of poly(U)•poly(A)\*poly(U) (Fig. 5, a ) shows  
6  
7 a large positive band in the 250-280 nm region and an adjacent weak negative band in the  
8  
9 wavelength range 230-250 followed by a small positive band below the 230 nm region.<sup>31</sup>  
10  
11 Notably, both Ru1 and Ru2 display no intrinsic CD signals because they are racemic  
12  
13 compounds. Furthermore, The RNA triplex displays no CD signs above 300 nm. Thus, for  
14  
15 the RNA triplex–Ru1/Ru2 system, any CD signals above 300 nm may be attributed to the  
16  
17 interaction of the complex with the triplex, and any changes below 300 nm could be due  
18  
19 either to the triplex induced CD (ICD) of the metal complex or the metal complex induced  
20  
21 perturbation of the RNA triplex spectrum. Fig. 5 indicated that the conformation of the  
22  
23 triplex was found to be perturbed in the presence of either Ru1 (Fig. 5, A) or Ru2 (Fig. 5,  
24  
25 B). As the interaction progressing the characteristic positive band of the RNA triplex in the  
26  
27 250–280 nm regions displayed obvious red shifts and decreases in ellipticity. Furthermore,  
28  
29 obvious induced CD was observed in 300-500 nm regions. In the case of Ru1, three new  
30  
31 bands at around 327, 352 and 476 nm were observed, whereas only one broad negative  
32  
33 band occurred at about 344 nm in the presence of Ru2. The results suggested that  
34  
35 Ru1–induced conformational changes of the RNA triplex are more obvious than Ru2,  
36  
37 which is also consistent with the above results.  
38  
39  
40  
41  
42  
43  
44  
45  
46  
47

### 48 **3.5. Thermal denaturation studies**

49  
50 A thermal denaturation experiment is an effective way to determine the stability of nucleic  
51  
52 acid duplexes and triplexes.<sup>42</sup> It's well established that a stacking interaction of intercalated  
53  
54 molecule as well as the neutralization of the phosphate charges through external binding may  
55  
56  
57  
58  
59  
60

1  
2  
3  
4  
5  
6  
7  
8  
9  
10  
11  
12  
13  
14  
15  
16  
17  
18  
19  
20  
21  
22  
23  
24  
25  
26  
27  
28  
29  
30  
31  
32  
33  
34  
35  
36  
37  
38  
39  
40  
41  
42  
43  
44  
45  
46  
47  
48  
49  
50  
51  
52  
53  
54  
55  
56  
57  
58  
59  
60

increase the melting temperature of nucleic acid duplexes and triplexes. In particular, information regarding the specificity of binding of small molecules to the Hoogsteen base-paired third strand poly(U) or to the Watson–Crick base-paired duplex poly(U)•poly(A) of triplexes can be obtained by thermal denaturation experiment.<sup>44</sup> Concerning the triplex poly(U)•poly(A)\*poly(U)-free Ru1 and Ru2, the third strand poly(U) separation from the triplex occurs at about 37.5 °C, while the duplex strand poly(U)•poly(A) separation occurs at around 45.6 °C, which is in agreement with the literature data.<sup>31</sup>

To explore Ru1 and Ru2 effect on the stability of the triplex, the thermal denaturation experiments were carried out. The denaturation curves at different  $C_{Ru}/C_{UAU}$  ratios were presented in Fig. 6, and the quantitative data on the melting temperatures were summarized in Table 2. The results indicated that the binding stabilized the Hoogsteen base paired third strand by about 7.6 and 6.5 °C for Ru1 and Ru2, respectively. The stabilization temperature of the third strand enhanced by Ru1 was slightly higher than that by Ru2, suggesting a delayed strand separation with bound Ru1 under the same conditions. In addition, the results also suggest that both Ru1 and Ru2 tend to slightly destabilize the Watson–Crick base-paired duplex of the triplex, reflecting the two complexes binding more strongly to the Hoogsteen base-paired third strand than to the Watson–Crick base-paired duplex under the present experiments. Notably, the effects of Ru1 and Ru2 on the stabilization of the triplex are different from ethidium,<sup>13</sup> some alkaloids,<sup>18</sup> proflavine and its complex Pt-proflavine.<sup>31</sup> The melting experiments reveal that ethidium, PR and its metal complex PtPR, tend to strongly destabilize the third strand poly(U) and stabilize the duplex poly(U)•poly(A), whereas some alkaloids, such as berberine, palmatine and coralyne, stabilize the Hoogsteen base-paired third strand of the triplex with no obvious affecting on the stability of the duplex. Recent studies of

1  
2 the interaction mechanisms of coralyne with poly(U)•poly(A)\*poly(U) confirm that coralyne  
3  
4 tends to stabilize the triplex structure because of this small molecule being able to induce the  
5  
6 triplex-to-duplex conversion and also the duplex-to-triplex conversion.<sup>14b</sup> These results  
7  
8 further suggest that the effects of small molecules on the stabilization of RNA triplexes are  
9  
10 complicated and sensitive to their structural features and interaction processes.  
11  
12  
13  
14

### 15 **3.6. Theoretical explanation on the interaction difference between Ru1 and Ru2**

16  
17 The above experimental results confirm that the binding affinity for Ru1 is slightly greater  
18  
19 than that for Ru2, which results in Ru1 displaying a stronger stabilization of the triplex  
20  
21 poly(U).poly(A)\*poly(U) in comparison with Ru2. Since the intercalative ligands of Ru1 and  
22  
23 Ru2 are the same, the differences in the binding affinities for the two complexes may be  
24  
25 attributed to the ancillary ligand effects. Previous investigations indicate that the  
26  
27 hydrophobicity of a ancillary ligand is one of many important factors governing the binding  
28  
29 affinities of Ru(II) polypyridine complexes to nucleic acids.<sup>44</sup> Obviously, concerning Ru1 and  
30  
31 Ru2 here, the hydrophobicity of bpy and phen may not be the main factor effect on the triplex  
32  
33 binding behaviors. Concerning Ru1 and Ru2 here, the hydrophobicity of the ancillary ligand  
34  
35 bpy is weaker than that of phen. If the hydrophobicity of the ancillary ligand is a main factor  
36  
37 governing the binding affinities for Ru1 and Ru2, the binding affinity for Ru1 should be  
38  
39 smaller than that for Ru2, which is opposite to the experimental results. Therefore, we  
40  
41 presume that the difference in the binding affinities of the two complexes can not be attributed  
42  
43 to the ancillary ligand effects, although Ru1 and Ru2 contain the same the intercalative ligand  
44  
45 btip and different ancillary ligands (bpy and phen). Herein, the situation of Ru1 and Ru2 is  
46  
47 similar to Ru(II) complexes  $[\text{Ru}(\text{bpy})_2(\text{actatp})]^{2+}$  and  $[\text{Ru}(\text{phen})_2(\text{actatp})]^{2+}$  (actatp =  
48  
49  
50  
51  
52  
53  
54  
55  
56  
57  
58  
59  
60

1  
2 acenaphthereno[1,2-*b*]-1,4,8,9-tetraazariphenylene) binding with calf thymus DNA.<sup>45</sup> The  
3  
4 result reported by Ji and his coworkers indicated that the binding affinity for  
5  
6  
7  
8  
9  
10  
11  
12  
13  
14  
15  
16  
17  
18  
19  
20  
21  
22  
23  
24  
25  
26  
27  
28  
29  
30  
31  
32  
33  
34  
35  
36  
37  
38  
39  
40  
41  
42  
43  
44  
45  
46  
47  
48  
49  
50  
51  
52  
53  
54  
55  
56  
57  
58  
59  
60

[Ru(bpy)<sub>2</sub>(actatp)]<sup>2+</sup> was bigger than that for [Ru(phen)<sub>2</sub>(actatp)]<sup>2+</sup>. This result suggest that the ancillary ligands governing Ru(II) complexes binding with nucleic acids can not t be absolute, even Ru(II) complexes contain the same intercalative ligand.

Notably, studies on the interactions of aromatic small molecules with DNA reflect that  $\pi$ - $\pi$  stacking (intermolecular force) plays a dominant role in the intercalations and the binding affinities. In general, the base pairs of DNA are electron-donors and aromatic molecules as intercalators are electron-acceptors.<sup>46,47</sup> Based on the frontier molecular orbital theory, two factors play a critical role in the binding affinities of aromatic molecules with DNA.<sup>48-50</sup> One is the planarity area of intercalators because the larger planarity area is advantageous to the interaction between DNA and intercalators, another is the lowest unoccupied molecular orbital (LUMO) energies because lower LUMO energies of DNA intercalators are advantageous to accepting the electrons from the base pairs of DNA. In addition, the reported HOMO and NHOMO (the next HOMO) energies of the CG/CG stacking model calculated with the density function theory (DFT) methods are -1.27 and -2.08 eV, respectively.<sup>47</sup> As well-established, due to the Hoogsteen base pairings, the stability of RNA triplexes is much lower than DNA.<sup>6,7</sup> Thus, we may reasonably conclude that the HOMO energies of RNA triplexes are much higher than that of DNA, namely, the HOMO energies of the AU/UA stacking model of RNA triplexes calculated with DFT method should be higher than the value of -1.27 eV. If so, the trends in the interactions of Ru1 and Ru2 with the triplex could be also explained by DFT methods.

Although the crystal structures of Ru1 and Ru2 have not been obtained here, the

1  
2  
3  
4  
5  
6  
7  
8  
9  
10  
11  
12  
13  
14  
15  
16  
17  
18  
19  
20  
21  
22  
23  
24  
25  
26  
27  
28  
29  
30  
31  
32  
33  
34  
35  
36  
37  
38  
39  
40  
41  
42  
43  
44  
45  
46  
47  
48  
49  
50  
51  
52  
53  
54  
55  
56  
57  
58  
59  
60

DFT-optimized structures confirm that the planarities of the intercalative ligands btip in the two complexes are different: for btip in Ru1 and Ru2, the dihedral angles of N(4)–C(5)–C(6)–S(7) are 0.2630 and 0.3751 ° (Fig. 7 and Table 3), respectively. Therefore, the better planarity of btip in Ru1 is more advantageous to the  $\pi$ - $\pi$  stacking interaction between Ru1 and the triplex RNA, which makes Ru1 insert the bases of the triplex more deeply than Ru2. On the other hand, the DFT calculations indicate that the energies of frontier molecular orbitals of the two metal complexes changes by the change in the N(4)–C(5)–C(6)–S(7) dihedral angles for Ru1 and Ru2 (Fig. 8 and Table 3), respectively. From Fig. 8 and Table 3, we can clearly see that the energies of LUMO and L + x (L= LUMO; x = 1, 2, etc.) of Ru1 are all smaller than those of Ru2. According to the frontier MO theory,<sup>48–50</sup> the lower energies of LUMO and L + x are more advantageous to Ru1 accepting the electrons offered from the base pairs of the triplex RNA, which can weaken the electrostatic repulsion between the third-strand and the duplex of the triplex RNA. Synthetically considering the two factors, the slight difference in the binding affinity and increase of the triplex stabilization for Ru1 and Ru2 could be reasonably explained.

#### 4. Conclusions

On the whole, the results from this work suggest that Ru1 and Ru2 can bind with the RNA triplex via intercalation and enhance the stabilization of the Hoogsteen base paired third strand. To some extent, the two complexes tend to destabilize the Watson–Crick base-paired duplex of the triplex, reflecting that both complexes are likely to bind with the Hoogsteen base-paired third strand more strongly than the Watson–Crick base-paired duplex under the present experiments. Combined with the DFT calculations, we presume that the slight binding

1  
2 difference in Ru1 and Ru2 may be attributed to the planarity of the intercalative ligand btip  
3  
4 and the LUMO level of Ru1 and Ru2, instead of the polarity effect of the ancillary ligands bpy  
5  
6 and phen. This study further advances our knowledge on the triplex RNA-binding by metal  
7  
8 complexes, particularly Ru(II) complexes.  
9  
10

## 11 12 13 14 **Acknowledgments**

15  
16 Supported by Funds for National Natural Science Foundation of China (21071120 and  
17  
18 21371146), Hunan Provincial Natural Science Foundation of China (12JJ2011) and the Key  
19  
20 Project of Chinese Ministry of Education (212127).  
21  
22  
23

## 24 25 26 **References**

- 27  
28 1 G. Felsenfeld, D. R. Davies and A. Rich, *J. Am. Chem. Soc.*, 1957, **79**, 2023–2024.  
29  
30 2 H. E. Moser and P. B. Dervan, *Science*, 1987, **238**, 645–650.  
31  
32 3 T. L. Doan, L. Perrouault, M. Chassignol, T. T. Nguyen and C. S. Hélène, *Nucleic Acids Res.*,  
33  
34 1987, **15**, 8643–8659.  
35  
36 4 A. Jain, A. Bacolla, P. Chakraborty, F. Grosse and K. M. Vasquez, *Biochemistry*, 2011, **49**,  
37  
38 6992–6999.  
39  
40 5 N. K. Conrad, *Wiley Interdiscip Rev. RNA*, 2014, **5**, 15–29.  
41  
42 6 (a) L. A. Christensen, R. A. Finch, A. J. Booker and K. M. Vasquez, *Cancer Res.*, **2006**, **66**,  
43  
44 4089–4094; (b) A. F. Buske, J. S. Mattick and T. L. Bailey, *RNA Biol.*, 2011, **8**, 427–439.  
45  
46 7 (a) P. Gupta, O. Muse and E. Rozners, *Biochemistry*, 2012, **51**, 63–73; (b) M. Li, T.  
47  
48 Zengeya and E. Rozners, *J. Am. Chem. Soc.*, 2010, **132**, 8676–8681.  
49  
50 8 (a) D. P. Arya, R. L. Coffee, Jr., and I. Charles, *J. Am. Chem. Soc.* 2001, **123**, 11093–11094;  
51  
52  
53  
54  
55  
56  
57  
58  
59  
60

- 1  
2 (b) D. P. Arya, L. Micovic, I. Charles, R. L. Coffee, Jr., B. Willis and L. Xue, *J. Am. Chem.*  
3  
4 *Soc.*, 2003, 125, 3733–3744.  
5  
6  
7 9 G. N. Ben, Z. Chao, S. R. Gerrard, K. R. Fox and T. Brown, *Chembiochem*, 2009, **10**,  
8  
9 1839–1851.  
10  
11 10 O. Doluca, A. S. Boutorine and V. V. Filichev, *Chembiochem*, 2011, **12**, 2365–2374.  
12  
13 11 D. Bhowmik and G. S. Kumar, *Mol. Biol. Rep.*, 2013, **40**, 5439–5450.  
14  
15 12 D. P. Arya, *Acc. Chem. Res.*, 2011, **44**, 134–146.  
16  
17 13 D. Bhowmik, S. Das, M. Hossain, L. Haq and G. S. Kumar, *PLoS ONE*, 2012, **7**,  
18  
19 e37939–e37939.  
20  
21 14 (a) H. J. Lozano, B. García, N. Busto and J. M. Leal, *J. Phys. Chem. B.*, 2013, **117**, 38–48;  
22  
23 (b) F. J. Hoyuelos, B. García, J. M. Leal, N. Busto, T. Biver, F. Secco and M. Venturinib,  
24  
25 *Phys. Chem. Chem. Phys.*, 2014, **16**, 6012–6018.  
26  
27 15 B. García, J. M. Leal, V. Paiotta, R. Ruiz, F. Secco and M. Venturini, *J. Phys. Chem. B.*,  
28  
29 2008, **112**, 7132–7139.  
30  
31 16 L. F. Tan, J. Liu , J. L. Shen, X. H. Liu, L. L. Zen and L. H. Jin, *Inorg. Chem.*, 2012, **51**,  
32  
33 4417–4419.  
34  
35 17 L. F. Tan, L. J. Xie and X. N. Sun, *J. Biol. Inorg. Chem.*, 2013, **18**, 71–80.  
36  
37 18 R. Sinha and G. S. Kumar, *J. Phys. Chem. B.*, 2009, **113**, 13410–13420.  
38  
39 19 H. J. Xi, E. Davis, N. Ranjan, L. Xue, D. Hyde-Volpe and D. P. Arya, *Biochemistry*, 2011,  
40  
41 **50**, 9088–91113.  
42  
43 20 A. K. Shchyolkina, E. N. Timofeev, Y. P. Lysov, V. L. Florentiev, T. M. Jovin, and D. J.  
44  
45 Arndt-Jovin, *Nucleic Acids Res.*, 2001, **29**, 986–995.  
46  
47 21 M. Polak and N. V. Hud, *Nucleic Acids Res.*, 2002, **30**, 983–992.  
48  
49  
50  
51  
52  
53  
54  
55  
56  
57  
58  
59  
60

- 1  
2  
3 22 E. A. Lehrman and D. M. Crothers, *Nucleic Acids Res.*, 1977, **4**, 1381–1392.  
4  
5 23 B. Garcia, J. M. Leal, V. Paiotta, S. Ibeas, R. Ruiz, F. Secco and M. Venturini, *J. Phys.*  
6  
7 *Chem. B.*, 2006, **110**, 16131–16138.  
8  
9  
10 24 G. L. Liao, X. Chen, L. N. Ji and H. Chao, *Chem. Commun.*, 2012, **48**, 10781–10783.  
11  
12 25 T. Very, S. Despax, P. Hébraud, A. Monaria and X. Assfelda, *Phys. Chem. Chem. Phys.*,  
13  
14 2012, **14**, 12496–12504.  
15  
16  
17 26 Y. Y. Xie, H. L. Huang, J. H. Yao, G. J. Lin, G. B. Jiang and Y. J. Liu, *Eur. J. Med. Chem.*,  
18  
19 2012, **63**, 603–610.  
20  
21  
22 27 M. Yamada, Y. Tanaka, Y. Yoshimoto, S. Kuroda and I. Shimao, *Bull. Chem. Soc. Jpn.*,  
23  
24 1992, **65**, 1006–1011.  
25  
26  
27 28 B. P. Sullivan, D. J. Sullivan and T. J. Meyer, *Inorg. Chem.*, 1978, **17**, 3334–3341.  
28  
29  
30 29 V. Buckin, H. Tran, V. Morozov and L. A. Marky, *J. Am. Chem. Soc.*, 1996, **118**,  
31  
32 7033–7039.  
33  
34  
35 30 R. Sinha and G. S. Kumar, *J. Phys. Chem. B.*, 2009, **113**, 13410–13420.  
36  
37  
38 31 S. Das, G. S. Kumar, A. Ray and M. Maiti, *J. Biomol. Struct. Dyn.*, 2003, **20**, 703–714.  
39  
40  
41 32 L. F. Tan, F. Wang, H. Chao. *Helv. Chim. Acta.*, 2007, **90**, 205–215.  
42  
43  
44 33 M. T. Carter, M. Rodriguez and A.J. Bard, *J. Am. Chem. Soc.*, 1989, **111**, 8901–8911.  
45  
46  
47 34 M. J. Frisch, G. W. Trucks, H. B. Schlegel, G. E. Scuseria, M. A. Robb, J. R. Cheeseman, V.  
48  
49 G. Zakrzewski, J. A. Montgomery, R. E. Stratmann, J. C. Burant, S. Dapprich, J.M. Millam,  
50  
51 A. D. Daniels, K. N. Kudin, M. C. Strain, O. Farkas, J. Tomasi, V. Barone, M. Cossi, R.  
52  
53 Cammi, B. Mennucci, C. Pomelli, C. Adamo, S. Clifford, J. Ochterski, G. A. Petersson, P. Y.  
54  
55 Ayala, Q. Cui, K. Morokuma, D. K. Malick, A. D. Rabuck, K. Raghavachari, J. B.  
56  
57 Foresman, J. Cioslowski, J. V. Ortiz, A. G. Baboul, B. B. Stefanov, G. Liu, A. Liashenko, P.  
58  
59  
60

- 1  
2 Piskorz, I. Komaromi, R. Gomperts, R.L. Martin, D.J. Fox, T. Keith, M.A. Al-Laham, C.Y.  
3  
4 Peng, A. Nanayakkara, M. Challacombe, P. M. W. Gill, B. Johnson, W. Chen, M. W. Wong,  
5  
6 J. L. Andres, C. Gonzalez, M. Head-Gordon, E. S. Replogle and J. A. Pople,  
7  
8 GAUSSIAN-98, Revision A.11.4, Gaussian, Inc., Pittsburgh, PA, 2002.  
9  
10  
11  
12 35 J. B. Foresman, Æ. Frisch, Exploring Chemistry with Electronic Structure Methods, second  
13  
14 ed., Gaussian Inc., Pittsburgh, PA, 1996.  
15  
16  
17 36 P. J. Hay and W. R. Wadt, *J. Chem. Phys.* 1985, **82**, 270–283.  
18  
19  
20 37 W. R. Wadt and P. J. Hay, *J. Chem. Phys.* 1985, **82**, 284–298.  
21  
22  
23 38 A. Juris, V. Balzani, F. Barigelletti, S. Campagna, P. Belser and A. V. Zelewsky, *Coord.*  
24  
25 *Chem. Rev.*, 1998, **84**, 85–277.  
26  
27  
28 39 G. Schaftenaar, J.H. Noordik, *J. Comput. Aid. Mol. Design.*, 2000, **14**, 123–134.  
29  
30  
31 40 A. Kabir and G. S. Kumar, *Mol. BioSyst.*, 2014, **10**, 1172–1183.  
32  
33 41 S. Banerjee, E. B. Veale, C. M. Phelan, S. A. Murphy, G. M. Tocci, L. J. Gillespie, D. O.  
34  
35 Frimannsson, J. M. Kelly, and T. Gunnlaugsson, *Chem. Soc Rev.*, 2013, 42, 1601–1618.  
36  
37  
38 42 L. S. Lerman, *J. Mol. Biol.*, 1961, **18–303**, 18–30.  
39  
40  
41 43 S. D. Choi, M. S. Kim, S. K. Kim, P. Lincoln, E. Tuite and B. Nordén, *Biochemistry*, 1997,  
42  
43 **36**, 214–223.  
44  
45  
46 44 L. N. Ji , X. H. Zou, J. G. Liu, *Coord. Chem. Rev.*, 2001, **216–217**, 513–536.  
47  
48  
49 45 H. Deng, H. Xu, Y. Yang, H. Li, H. Zou, L. H. Qu , L. N Ji, *J. Inorg. Biochem.*, 2003, **97**,  
50  
51 207–214.  
52  
53  
54 46 D. Reha, M. Kabelac, F. Ryjacek, J. Sponer, J.E. Sponer, M. Elstner, S. Suhai, P. Hobza, *J.*  
55  
56 *Am. Chem. Soc.*, 2002, 124, 3366–3376.  
57  
58  
59 47 N. Kurita, K. Kobayashi, *Computat. Chem.*, 2000, **24**, 351–357.  
60

1  
2 48 K. Fukui, T. Yonezawa, H. Shingu, *J. Chem. Phys.*, 1952, **20**, 722–725.  
3

4  
5 49 G. Klopman, *J. Am. Chem. Soc.*, 1968, **90**, 223–234.  
6

7 50 I. Fleming, *Frontier Orbital and Organic Chemical Reaction*, Wiley, New York, 1976.  
8  
9  
10  
11  
12  
13  
14  
15  
16  
17  
18  
19  
20  
21  
22  
23  
24  
25  
26  
27  
28  
29  
30  
31  
32  
33  
34  
35  
36  
37  
38  
39  
40  
41  
42  
43  
44  
45  
46  
47  
48  
49  
50  
51  
52  
53  
54  
55  
56  
57  
58  
59  
60

## Captions for Schemes and Figures

**Fig. 1.** Chemical structures of Ru1, Ru2 and the base pairing scheme in poly(U)•poly(A)\*poly(U) (symbols • and \* represent Watson-Crick and Hoogsteen base pairing).

**Fig. 2.** Representative absorption spectral changes of Ru1 (A) and Ru2 (B) in phosphate buffer (6 mmol/L Na<sub>2</sub>HPO<sub>4</sub>, 2 mmol/L NaH<sub>2</sub>PO<sub>4</sub>, 1 mmol/L Na<sub>2</sub>EDTA, 19 mmol/L NaCl, pH 7.0) at 20 °C in the absence and presence of poly(U)•poly(A)\*poly(U). [Ru1] = [Ru2] = 20 μM, [UAU] = 0–126 μM {UAU stands for poly(U)•poly(A)\*poly(U)}. The arrows show the absorbance changes upon increasing poly(U)•poly(A)\*poly(U) concentrations.

**Fig.3.** Representative fluorescence emission spectra of Ru1 (A) and Ru2 (B) treated with poly(U)•poly(A)\*poly(U). [Ru1] = [Ru2] = 1.0 μM, [UAU] = 0–93 μM. The arrows show the emission intensity changes upon increasing poly(U)•poly(A)\*poly(U) concentrations. Solution conditions are the same as those described in the legend of Fig. 2.

**Fig. 4.** Circular dichroism spectra of poly(U)•poly(A)\*poly(U) (a, 50.0 μM) treated with Ru1 (A) and Ru2 (B), respectively. [Ru]/[UAU] = 0–0.35; Red lines: the Ru-free RNA triplex (Ru stands for Ru1 and Ru2, respectively). The solution conditions are the same as those described in the legend of Fig. 2.

**Fig. 5.** Viscometric Ru1 (■) Ru2 (●) and titrations of poly(U)•poly(A)\*poly(U) at 20 °C. [UAU] = 153 μM. Solution conditions are the same as those described in the legend of Fig. 2.

**Fig. 6.** Melting curves at 260 nm of poly(U)•poly(A)\*poly(U) (32.1 μM) and its complexation with Ru1 (A) and Ru2 (B) at different [Ru]/[UAU] ratios. Solution conditions are the same as those described in the legend of Fig. 2, and [Na<sup>+</sup>] = 35 mM.

**Fig. 7.** The DFT-optimized structures and visualization of the orbitals of Ru1 (left) and Ru2 (right).

**Fig. 8** Some related frontier molecular orbital stereographs of complexes of Ru1 and Ru2.

**Table 1.** Binding constants ( $K_b$ ), average binding site size ( $s$ ), hypochromicity ( $H$ ) and bathochromic shifts of Ru1 and Ru2.

Complexes	$\lambda_{max,free}$ (nm)	$\lambda_{max,bound}$ (nm)	$\Delta\lambda^a$ (nm)	$H^b$ (%)	$K_b^c$ ( $\times 10^6 M^{-1}$ )	$s^d$
Ru1	463	469	6	16.72	$2.23 \pm 0.41$	$1.31 \pm 0.03$
Ru2	464	467	3	15.60	$1.59 \pm 0.46$	$0.85 \pm 0.04$

<sup>a</sup>  $\Delta\lambda$  represents the difference in wavelength of the MLCT band of the metal complex between free and completely bound the triplex states.

<sup>b</sup>  $H = 100 \times (A_{free} - A_{bound})/A_{free}$  ( $A$  is the absorbance).

<sup>c</sup>  $K_b$  was determined by monitoring the changes of absorption at the MLCT bands.

<sup>d</sup>  $s$  is an average binding size.

**Table 2.** Melting Temperature ( $^{\circ}\text{C}$ ) of poly(U)•poly(A)\*poly(U) in the absence and presence of Ru1 and Ru2, respectively.  $[\text{Na}^+] = 35 \text{ mM}$ .

Complexes	$C_{\text{Ru}}/C_{\text{UAAU}}$	$T_{\text{m1}}^{\text{a}}$ ( $^{\circ}\text{C}$ )	$T_{\text{m2}}^{\text{b}}$ ( $^{\circ}\text{C}$ )	$\Delta T_{\text{m1}}$	$\Delta T_{\text{m2}}$
poly(U)•poly(A)*poly(U)	0	37.5	45.6	–	–
poly(U)•poly(A)*poly(U)+ Ru1	0.01	40.1	46.3	2.6	0.7
	0.02	40.4	45.7	2.9	0.1
	0.05	44.6	–	7.1	–
	0.10	45.0	–	7.5	–
poly(U)•poly(A)*poly(U)+ Ru2	0.01	39.3	46.0	1.8	0.4
	0.02	41.6	45.5	4.1	-0.1
	0.05	43.8	–	6.3	–
	0.10	44.2	–	6.7	–

<sup>a,b</sup>  $T_{\text{m1}}$  and  $T_{\text{m2}}$  are the thermal melting temperatures corresponding to triplex to duplex and duplex to single strand transitions, respectively.

**Table 3.** Dihedral angles  $\theta$  ( $^\circ$ ) and some frontier molecular orbital energies ( $\epsilon_i/\text{eV}$ ) of complexes Ru1 and Ru2.

Title	$\theta$ ( $^\circ$ ) <sup>a</sup>	HOMO-2	HOMO-1	HOMO <sup>b</sup>	LUMO <sup>c</sup>	LUMO+1	LUMO+2	$\Delta\epsilon_{\text{L-H}}$ <sup>d</sup>
Ru1	0.2630	-10.7700	-9.7934	-9.4944	-7.4256	-7.3372	-7.1715	2.0688
Ru2	0.3751	-10.6786	-9.7483	-9.4509	-7.2673	-7.1720	-7.0858	2.1836

<sup>a</sup>) N(4)–C(5)–C(6)–S(7).

<sup>b</sup>) HOMO: the highest occupied molecular orbital; HOMO-1 = the next HOMO.

<sup>c</sup>) LUMO: the lowest unoccupied molecular orbital; LUMO+1: the next LUMO.

<sup>d</sup>)  $\Delta\epsilon_{\text{L-H}}$  = the energy difference between LUMO and HOMO.

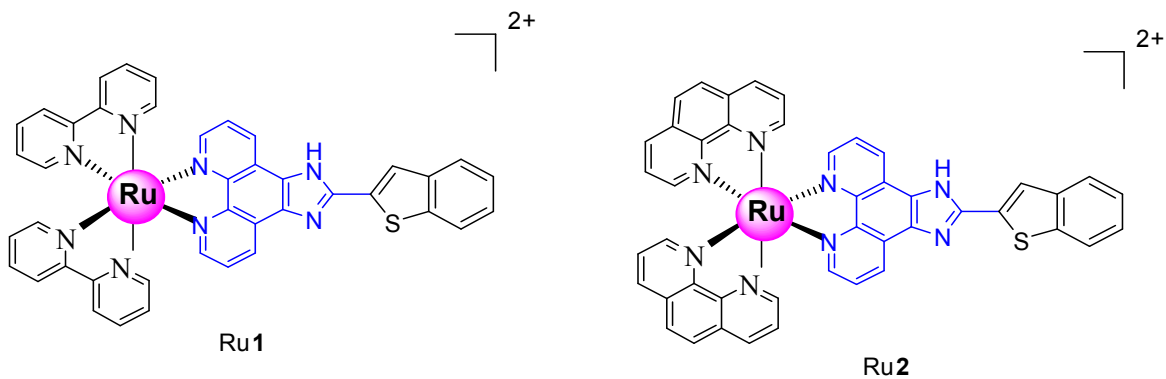
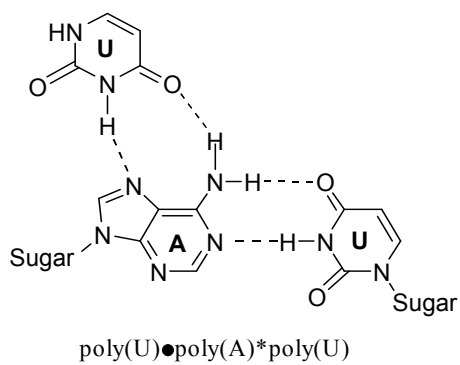


Fig. 1.

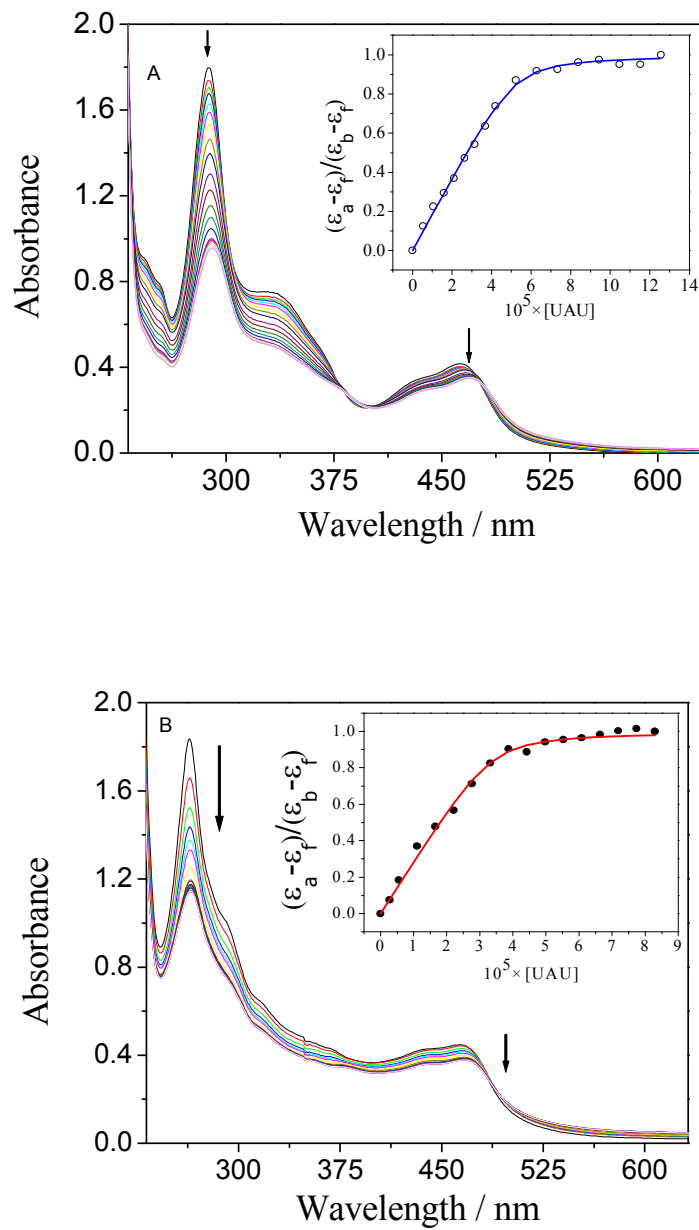
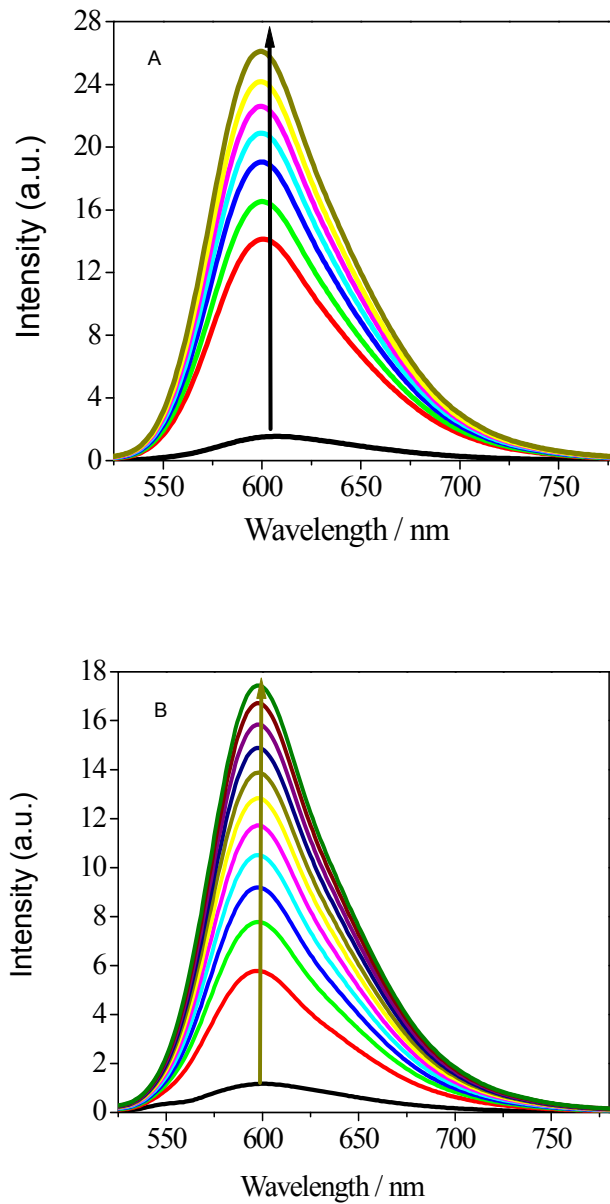


Fig. 2.



Metallomics Accepted Manuscript

Fig. 3.

1  
2  
3  
4  
5  
6  
7  
8  
9  
10  
11  
12  
13  
14  
15  
16  
17  
18  
19  
20  
21  
22  
23  
24  
25  
26  
27  
28  
29  
30  
31  
32  
33  
34  
35  
36  
37  
38  
39  
40  
41  
42  
43  
44  
45  
46  
47  
48  
49  
50  
51  
52  
53  
54  
55  
56  
57  
58  
59  
60

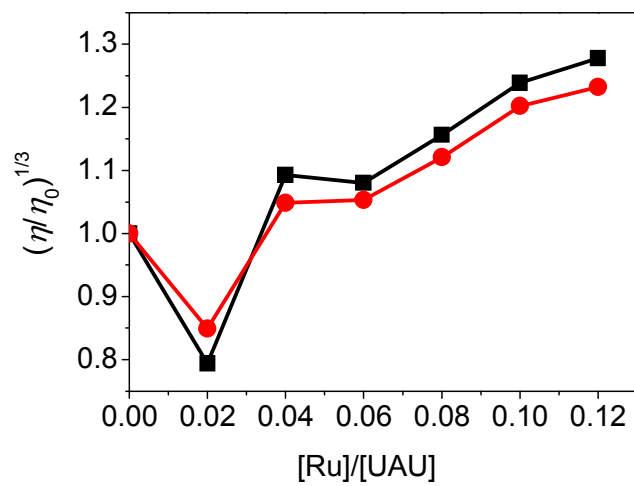


Fig. 4.

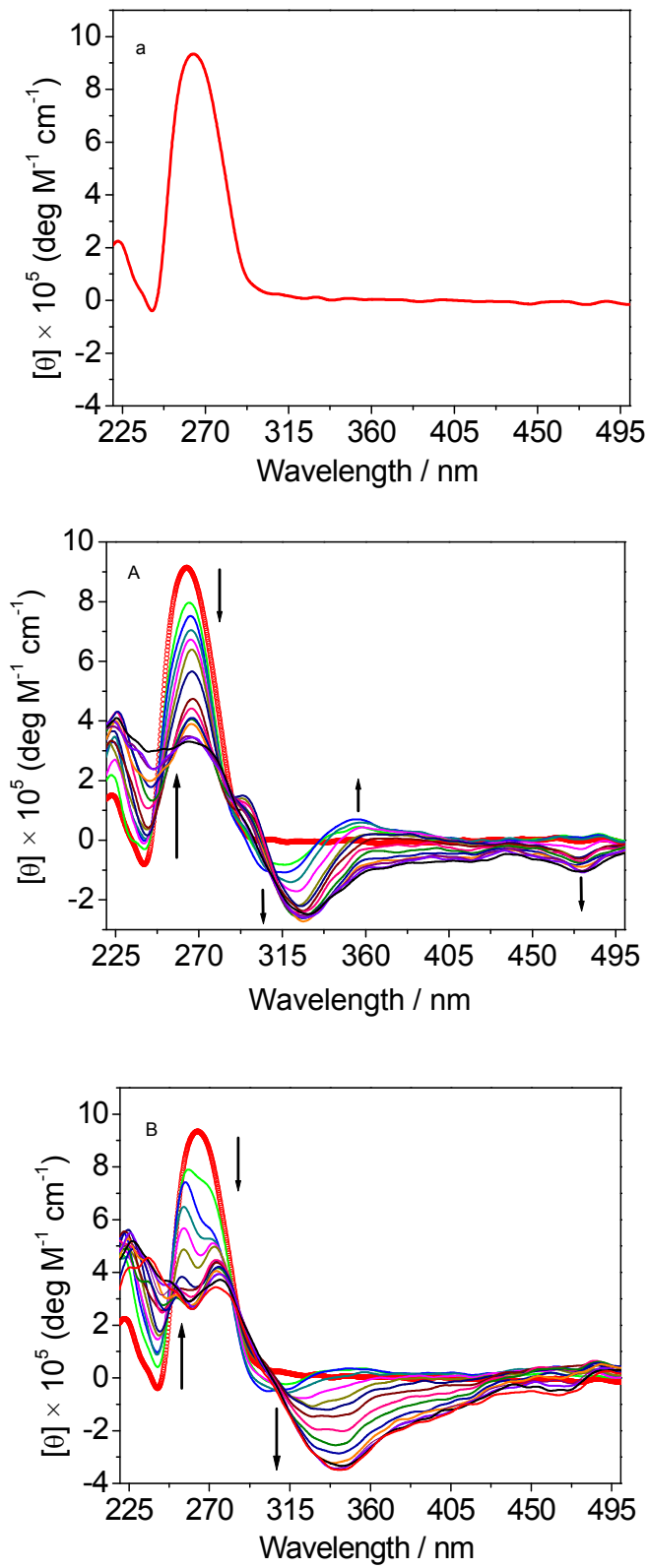


Fig. 5.

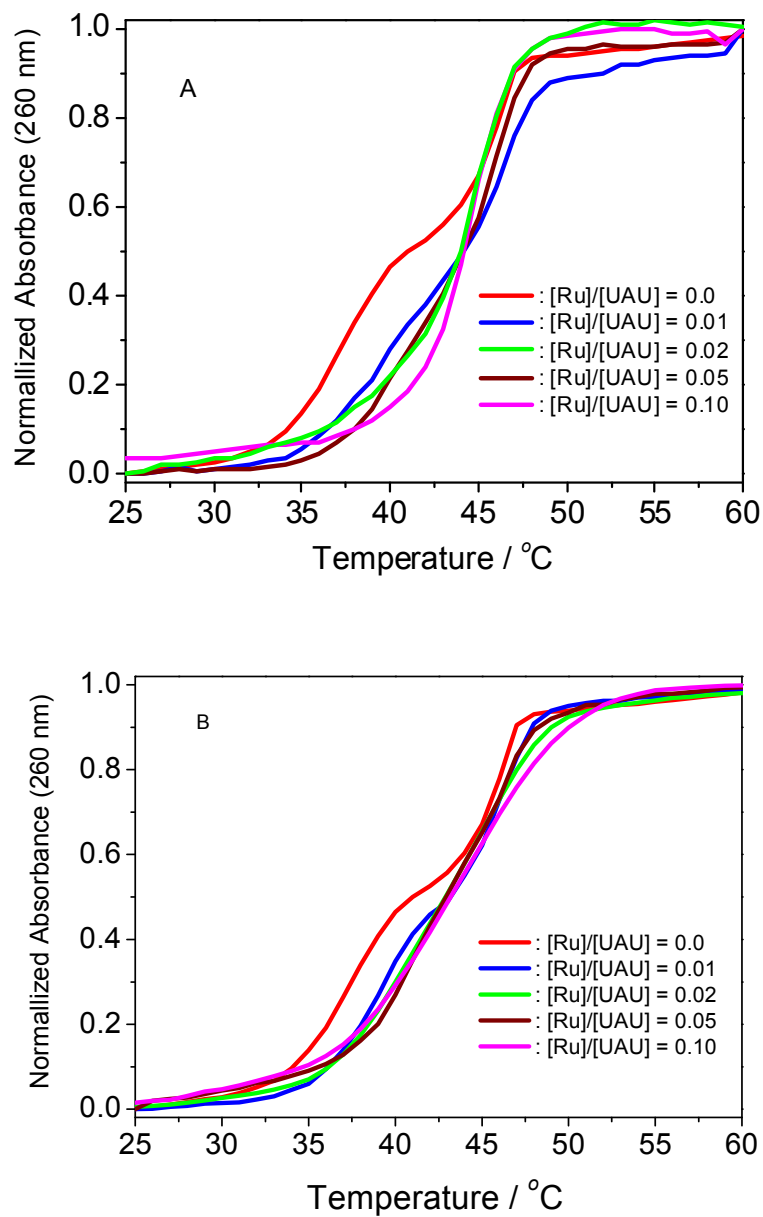


Fig. 6.

1  
2  
3  
4  
5  
6  
7  
8  
9  
10  
11  
12  
13  
14  
15  
16  
17  
18  
19  
20  
21  
22  
23  
24  
25  
26  
27  
28  
29  
30  
31  
32  
33  
34  
35  
36  
37  
38  
39  
40  
41  
42  
43  
44  
45  
46  
47  
48  
49  
50  
51  
52  
53  
54  
55  
56  
57  
58  
59  
60

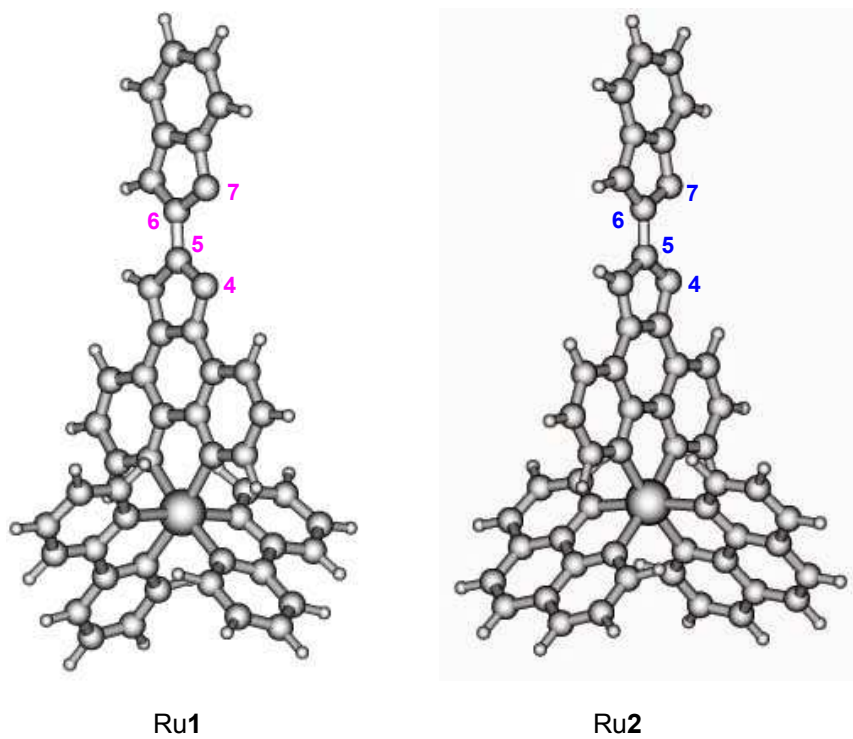


Fig. 7.

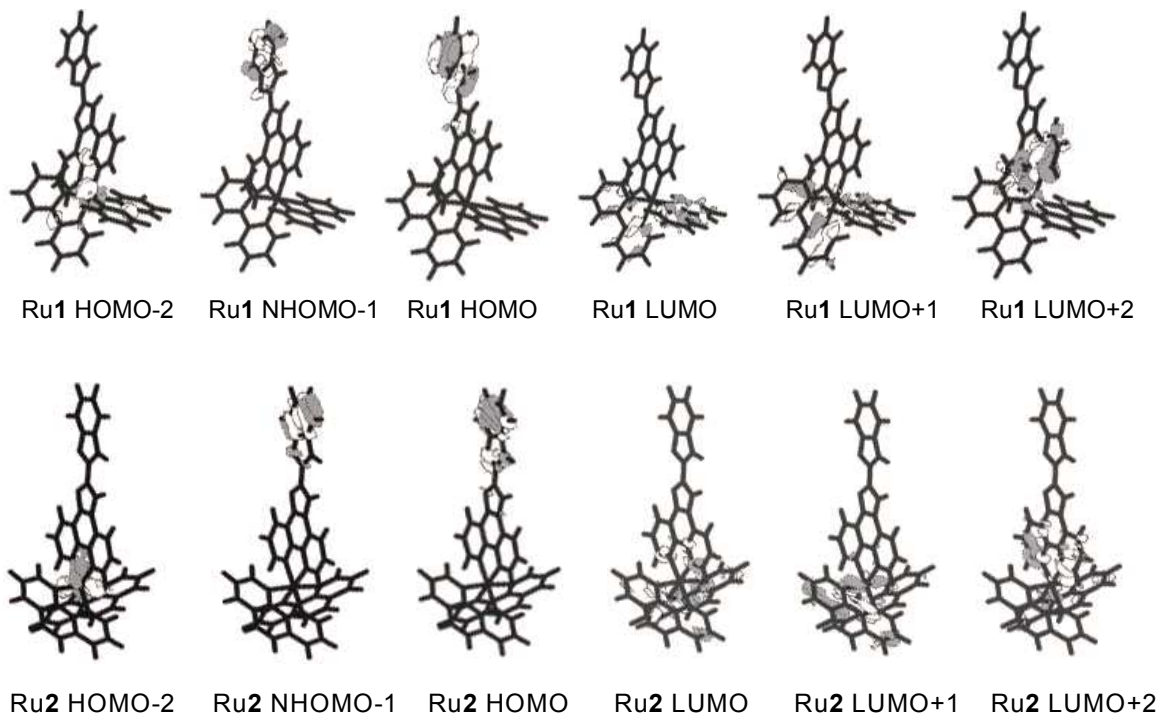
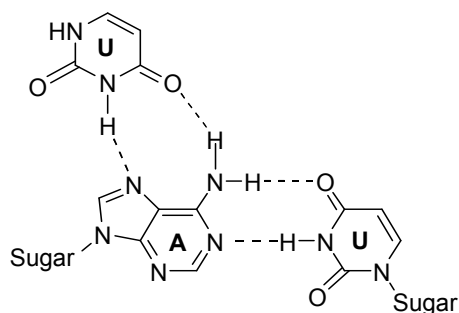
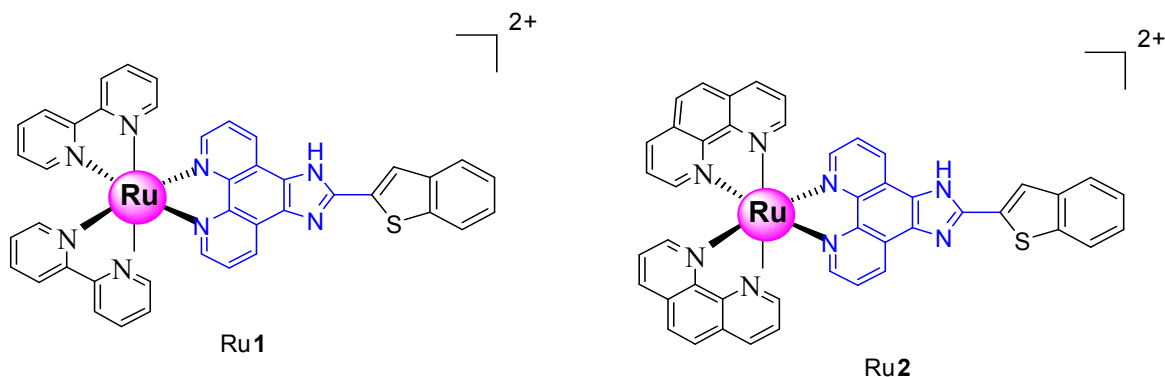


Fig. 8.

1  
2  
3  
4  
5  
6  
7  
8  
9  
10  
11  
12  
13  
14  
15  
16  
17  
18  
19  
20  
21  
22  
23  
24  
25  
26  
27  
28  
29  
30  
31  
32  
33  
34  
35  
36  
37  
38  
39  
40  
41  
42  
43  
44  
45  
46  
47  
48  
49  
50  
51  
52  
53  
54  
55  
56  
57  
58  
59  
60



poly(U)•poly(A)\*poly(U)



In this work, two Ru(II) complexes,  $[\text{Ru}(\text{bpy})_2(\text{btip})]^{2+}$  (Ru1) and  $[\text{Ru}(\text{phen})_2(\text{btip})]^{2+}$  (Ru2), have been synthesized and characterized. The binding properties of the two metal complexes with the triple RNA poly(U)•poly(A)\*poly(U) were studied by various biophysical and density functional theory methods. The main results obtained here suggest that the slight binding difference in Ru1 and Ru2 may be attributed to the planarity of the intercalative ligand and the LUMO level of Ru(II) complexes. This study further advances our knowledge on the triplex RNA-binding by metal complexes, particularly Ru(II) complexes.